Fourier transform emission spectroscopy of YH and YD: Observation of new A1Δ and B1Π electronic states

R. S. Ram, G. Li, and P. F. Bernath

Citation: J. Chem. Phys. **135**, 194308 (2011); doi: 10.1063/1.3659295
View online: http://dx.doi.org/10.1063/1.3659295
View Table of Contents: http://jcp.aip.org/resource/1/JCPSA6/v135/i19
Published by the American Institute of Physics.

Fourier transform emission spectroscopy of YH and YD: Observation of new $A^1\Delta$ and $B^1\Pi$ electronic states

R. S. Ram,[1,2,a)] G. Li,[1] and P. F. Bernath[1,3]
[1]*Department of Chemistry, University of York, Heslington, York YO10 5DD, United Kingdom*
[2]*Department of Chemistry, University of Arizona, Tucson, Arizona 85721, USA*
[3]*Department of Chemistry and Biochemistry, Old Dominion University, Norfolk, Virginia 23529 USA*

(Received 31 August 2011; accepted 19 October 2011; published online 18 November 2011)

The emission spectra of YH and YD molecules have been investigated in the 3600–12 000 cm^{-1} region using a Fourier transform spectrometer. Molecules were formed in an yttrium hollow cathode lamp operated with a continuous flow of a mixture of Ne and Ar gases, and YH and YD were observed together in the same spectra. A group of bands observed near 1 μm have been identified as 0-0 and 1-1 bands of the $A^1\Delta$-$X^1\Sigma^+$ and $B^1\Pi$-$X^1\Sigma^+$ transitions of YH and the 0-0 bands of the same two transitions for YD. The $A^1\Delta$ and $B^1\Pi$ states of YH are separated by only about 12 cm^{-1} and are involved in strong interactions. A perturbation analysis has been performed using the PGOPHER program to fit the two interacting electronic states and spectroscopic parameters for the $A^1\Delta$ and $B^1\Pi$ states, including the interaction matrix elements, have been obtained for the first time. © *2011 American Institute of Physics*. [doi:10.1063/1.3659295]

I. INTRODUCTION

In recent years, there has been considerable interest in the theoretical and experimental studies of transition metal containing molecules in order to unravel their complex spectra. These studies are also important to further our understanding of the role of *d* electrons in chemical bond formation. Diatomic transition metal hydrides provide the simplest model for the study of the metal-hydrogen bond in solid transition metal hydrides such as YH_x and LaH_x (x = 2,3), which are useful in modern technology due to their switchable optical properties.[1,2] These metal hydrides have the potential for technological utilization, for example, in solar cells.[3] Many transition metal elements are known to occur in S-type and M-type stars in the form of metal monoxides and mono-hydrides. Among yttrium containing molecules, YO has been identified in the spectra of S-type stars[4,5] and there is a possibility that YH may also be found.

The electronic spectra of YH and YD are known since 1977 when Bernard and Bacis[6] observed numerous bands in the 380–900 nm region and classified them into several electronic transitions involving singlet and triplet states. In the absence of singlet-triplet inter-combination transitions and reliable theoretical calculations, they assumed that the ground state of YH was a $^3\Delta$ state, by analogy with the then available erroneous assignments for ScH (Ref. 7) and LaH.[8] It has now been experimentally established that ScH (Refs. 9 and 10) and LaH (Ref. 11) have $^1\Sigma^+$ ground states. The assignment of YH ground state as a $^3\Delta$ state was contradicted by subsequent theoretical calculations by Langhoff *et al.*,[12] which predicted a $^1\Sigma^+$ ground state. A more recent extensive complete active space self-consistent field (CASSCF) calculation taking into account the second order configuration interaction (SOCI) and relativistic configuration interaction (RCI) was carried out by Balasubramanian and Wang.[13] This work also predicted a $^1\Sigma^+$ ground state for YH and a $^3\Pi$ state as the first excited state. A number of higher-lying excited electronic states were also predicted by this study.[13] These *ab initio* predictions for the ground and low-lying electronic states were later confirmed by experimental studies by Simard *et al.*[14] and Ram and Bernath[15,16] in which a number of low-lying excited electronic states (e.g., $a^3\Delta$, $C^1\Sigma^+$, $d0^+$, and $e^3\Phi$) were observed and characterized.[15]

Matrix infrared spectra of MH_x (M = Sc, Y, La, and x = 1,2,3) produced by the reaction of laser-ablated atoms with molecular hydrogen were studied by Wang *et al.*[17] The observed spectra were interpreted using density functional theory calculations. The fundamental frequency of YH in Ar and Ne matrices was observed at 1470.4 cm^{-1} and 1496.1 cm^{-1}, respectively, compared to the gas phase value of 1491.6995 cm^{-1} from Ram and Bernath.[15]

In the most recent studies Jakubek *et al.*[18,19] have investigated the complex spectra of YH and YD in the green and blue regions. In particular, a number of bands located in the 19 300–19 900 cm^{-1} region were studied by laser-induced fluorescence in a molecular beam source. In order to obtain rotational and Ω assignments, Stark measurements were obtained for the ground and four excited states using bands located in the green region. The electronic assignments for the observed states at 19 381.352 cm^{-1}($f^3\Pi_1$), 19 573 cm^{-1} ($D^1\Pi$), 19 574 cm^{-1} ($f^3\Pi_2$), and 19 742.734 cm^{-1} (f′1) were proposed on the basis of these studies. Two further higher-lying electronic states, $E0^+$ (23 213.3 cm^{-1}) and F1 (23 426.5 cm^{-1}), having transitions to the ground state were also identified from the study of the blue region bands.

In the present paper we report on the first observation of two lowest-lying singlet excited states, $A^1\Delta$ and $B^1\Pi$,

a)Author to whom correspondence should be addressed. Electronic mail: rr662@york.ac.uk.

which have transitions to the ground state near 1 μm. These two states have been predicted to be located at 10 992 and 12 685 cm^{-1} by Balasubramanian and Wang,[13] but were not observed to date. These two states have been found to interact strongly with each other and a perturbation analysis was performed to obtain spectroscopic constants.

II. EXPERIMENT

The new bands near 1 μm were observed in two spectra [#13 and #14, November 17, 1988] recorded by Sveneric Johansson at the National Solar Observatory at Kitt Peak. A careful inspection and analysis of bands near 10 000 cm^{-1} indicates that these bands belong to YH and YD, which were simultaneously observed in Johansson's spectra. The hollow cathode lamp, made by inserting yttrium foil in a hole in a copper block, was operated at 124 mA current and 220 V with a flowing mixture of 1.4 Torr of Ar and Ne. No additional H_2 or D_2 was required to make YH and YD. Presumably, the H_2 and D_2 required to form YH and YD were present in the lamp from previous experiments intended to make BiH/BiD and HoH/HoD molecules. The spectra were recorded using the 1-m Fourier transform spectrometer associated with the McMath–Pierce Solar Telescope of the National Solar Observatory. The spectra in the 3600–38 000 cm^{-1} spectral region were recorded in two parts. The 3600–12 000 cm^{-1} region was recorded at a resolution of 0.012 cm^{-1} by coadding four scans in about 60 min of integration. For this region the spectrometer was equipped with a UV beam splitter, GaAs filters, and InSb detectors. The 9000–38 000 cm^{-1} region was recorded at a resolution of 0.038 cm^{-1} by coadding four scans. This time the spectrometer was equipped with the UV beam splitter and mid-range Si diode detectors. As the YH and YD bands are located near 10 000 cm^{-1} where the sensitivity of the Si-diode detectors is low, the YH and YD bands are quite weak compared to those observed to shorter wavelengths. Therefore, we decided to use the measurements of the lines from the first spectrum in our final analysis. The spectral line positions were extracted from the observed spectra using a data reduction program called PC-DECOMP developed by J. Brault. The peak positions were determined by fitting a Voigt line shape function to each spectral feature. In addition to the YH and YD bands, the spectra also contained Y and Ne atomic lines. The spectra were calibrated using the measurements of Ne atomic lines made by Palmer and Engleman.[20] The absolute accuracy of the wavenumber scale is expected to be better than ± 0.003 cm^{-1}.

III. OBSERVATIONS AND ANALYSIS

In our previous investigation of YH (Ref. 15) and YD (Ref. 16) we had recorded the spectra in the 3500–14 500 cm^{-1} region. In these spectra we did not observe any bands near 1 μm because of the poor response of our optical system. The higher wavenumber region (>14 500 cm^{-1}) was not covered in our previous experiments. The spectra recorded by Johansson showed the presence of additional molecular features near 10 000 cm^{-1} and 19 600 cm^{-1}. The 19 600 cm^{-1} region has recently been characterized by Jakubek *et al.*[18,19] A detailed investigation of the 1 μm bands was carried out by comparing the combination differences from these bands to the values for the known electronic states of YH and YD. It was found that the 1 μm bands consist of two transitions having the ground state as their lower state. With the assistance of theoretical calculations of Balasubramanian and Wang,[13] these two transitions were assigned as $A^1\Delta$-$X^1\Sigma^+$ and $B^1\Pi$-$X^1\Sigma^+$. Although the $A^1\Delta$-$X^1\Sigma^+$ transition is forbidden, the $A^1\Delta$ state mixes with the $B^1\Pi$ state and the transition becomes allowed. The band origins of the two transitions are separated only by $\sim$12 cm^{-1}.

A. The 1 μm spectrum of YH

Two bands with origins near 9848 cm^{-1} and 9859 cm^{-1} have been assigned as the 0-0 bands of the $A^1\Delta$-$X^1\Sigma^+$ and $B^1\Pi$-$X^1\Sigma^+$ transitions, respectively. The $A^1\Delta$-$X^1\Sigma^+$ transition has a weaker R-head near 9853 cm^{-1}, while the $B^1\Pi$-$X^1\Sigma^+$ transition has strong Q- and R-heads near 9896 cm^{-1} and 10 046 cm^{-1}. Corresponding 1-1 bands are located near 9695 and 9697 cm^{-1}, respectively. The spectrum of each band consists of P, Q, and R branches with the Q branch being the most intense. The R and P branches have almost equal intensity in the bands of both transitions. The spectrum is complex because of unusual spacing in the R, Q, and P branches and the assignment was possible only by finding a match between the lower state combination differences with those of the $X^1\Sigma^+$ state. The $A^1\Delta$-$X^1\Sigma^+$ bands are somewhat weaker in intensity than the $B^1\Pi$-$X^1\Sigma^+$ bands. We have identified rotational lines up to R(29), Q(34), and P(26) in the $A^1\Delta$-$X^1\Sigma^+$ 0-0 band and R(34), Q(37), and P(29) in the $B^1\Pi$-$X^1\Sigma^+$ 0-0 band. The 1-1 band of both transitions is much weaker in intensity than the 0-0 bands and we have assigned the rotational lines up to R(18), Q(20), P(17) and R(16), Q(30), P(18) in the 1-1 bands of these two transitions, respectively.

B. The 1 μm spectrum of YD

The YD spectrum is about 30% of the intensity of the YH bands present in the same region. For YD, we were able to identify only the 0-0 bands of the $A^1\Delta$-$X^1\Sigma^+$ and $B^1\Pi$-$X^1\Sigma^+$ transitions, and the 1-1 bands could not be seen because of weak intensity. The vibrational assignment of the two 0-0 bands was made by comparing the lower state combination differences with the previously known values from Ram and Bernath.[16] The observed YH-YD isotope shifts for the 0-0 bands of the $A^1\Delta$-$X^1\Sigma^+$ and $B^1\Pi$-$X^1\Sigma^+$ transitions of the two isotopologues are 33 and 22 cm^{-1}, respectively, which compares well with corresponding values from other transitions. For example, a shift of about 27 cm^{-1} was observed for the 0-0 bands of the $C^1\Sigma^+$-$X^1\Sigma^+$ transition of YH (Ref. 15) and YD.[16] We have identified rotational lines up to R(20), Q(28), and P(19) and R(22), Q(28), and P(23) in the 0-0 bands of the $A^1\Delta$-$X^1\Sigma^+$ and $B^1\Pi$-$X^1\Sigma^+$ transitions, respectively. A portion of the 0-0 band of the $B^1\Pi$-$X^1\Sigma^+$ transition is presented in Figure 1, in which some rotational lines of the head-forming R branch of YH and YD have been marked.

After obtaining the correct J assignment in the P, Q, and R branches of different bands, attempts were made to fit the

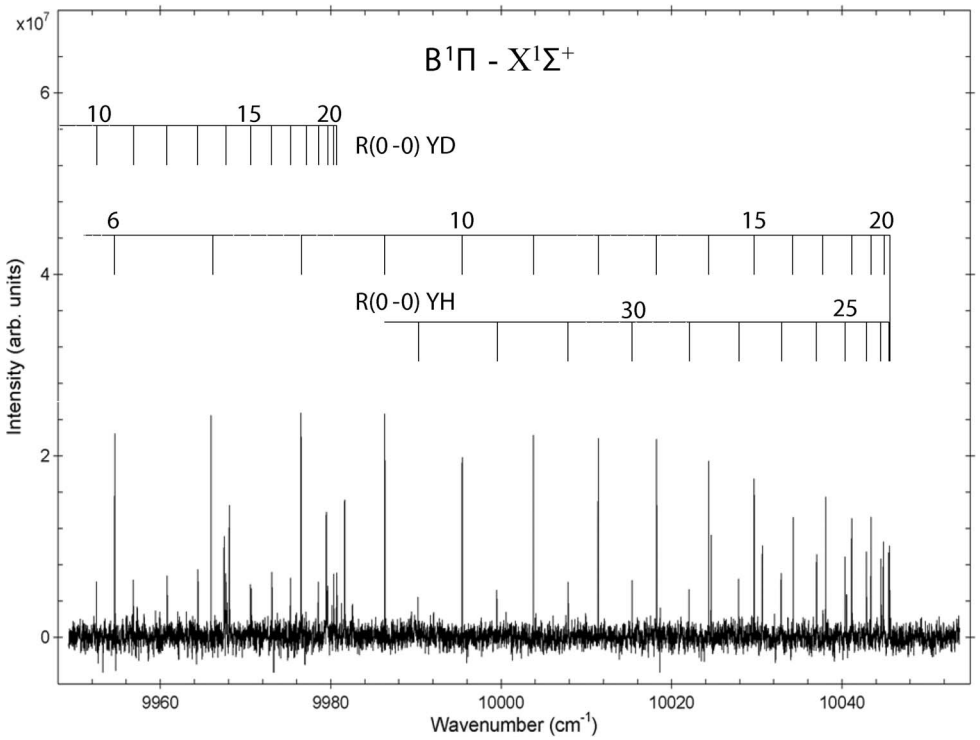

FIG. 1. A portion of the 0-0 band of the $B^1\Pi$-$X^1\Sigma^+$ transition, with some rotational lines in the R branches of YH and YD marked.

observed lines using the PGOPHER program, for convenience. The energy levels of the observed states are represented by the following expressions:

For the $X^1\Sigma^+$ state,

$$F_v(J) = T_v + B_vJ(J+1) - D_v[J(J+1)]^2 + H_v[J(J+1)]^3 + L_v[J(J+1)]^4 \quad (1)$$

and for the $B^1\Pi$ and $A^1\Delta$ states,

$$F_v(J) = T_v + B_vJ(J+1) - D_v[J(J+1)]^2 \pm \frac{1}{2}\{q_vJ(J+1) + q_{Dv}[J(J+1)]^2 + q_{Hv}[J(J+1)]^3\}. \quad (2)$$

Initial attempts were unsuccessful because of strong interaction between the close-lying $A^1\Delta$ and $B^1\Pi$ excited states. In order to take into account the interactions, a perturbation analysis was performed, details of which is provided in Sec. III C.

C. Perturbation analysis

The rotational (H_{rot}) and spin-orbit (H_{SO}) Hamiltonians in the molecular coordinate system are expressed as follows:[21]

$$H_{rot} = B(\mathbf{R})^2 = B(\mathbf{J}-\mathbf{L}-\mathbf{S})^2 = \left(J^2 - J_z^2\right) + B\left(S^2 - S_z^2\right) + B\left(L^2 - L_z^2\right) - B(J^+L^- + J^-L^+) - B(J^+S^- + J^-S^+) + B(L^+S^- + L^-S^+),$$

$$H_{SO} = A\mathbf{L}\cdot\mathbf{S} = AL_zS_z + \frac{1}{2}A\left(L^+S^- + L^-S^+\right),$$

where $J^\pm$, $L^\pm$, and $S^\pm$ are raising and lowering operators; J_z, L_z, S_z are the respective projections of **J**, **L**, **S** onto the internuclear axis; and all other constants have their usual meanings. Within the Born-Oppenheimer approximation, three terms in the rotational part of the Hamiltonian, H_{rot}, are neglected:[22]

1. $-B(J^+L^- + J^-L^+)$, which is the L-uncoupling operator.
2. $-B(J^+S^- + J^-S^+)$,which is the S-uncoupling operator.
3. $B(L^+S^- + L^-S^+)$, which causes spin-electronic homogeneous ($\Delta\Omega = 0$) perturbation.

For the $B^1\Pi$–$A^1\Delta$ interaction, all interaction terms vanish except for the L-uncoupling operator, $-B(J^+L^- + J^-L^+)$. In addition, approximate wavefunctions for the $1\sigma^2 2\sigma^1 1\delta^1$ $A^1\Delta$ state and the $1\sigma^2 2\sigma^1 1\pi^1$ $B^1\Pi$ state can be constructed as linear combinations of Slater determinants:

$$|^1\Delta_2\rangle = \frac{1}{\sqrt{2}}[|\sigma\alpha\delta^+\beta| - |\sigma\beta\delta^+\alpha|],$$

$$|^1\Pi_1\rangle = \frac{1}{\sqrt{2}}[|\sigma\alpha\pi^+\beta| - |\sigma\beta\pi^+\alpha|],$$

$$|^1\Delta_{-2}\rangle = \frac{1}{\sqrt{2}}[|\sigma\alpha\delta^-\beta| - |\sigma\beta\delta^-\alpha|],$$

$$|^1\Pi_{-1}\rangle = \frac{1}{\sqrt{2}}[|\sigma\alpha\pi^-\beta| - |\sigma\beta\pi^-\alpha|].$$

It is only necessary to consider the positive Ω values. Thus, the $B^1\Pi$–$A^1\Delta$ perturbation is characterized by the following

matrix element:

$$\begin{aligned}
&\langle B^1\Pi_1, v_B|H'|A^1\Delta_2, v_A\rangle \\
&= \langle B^1\Pi_1, v_B| - B(R)\, J^+L^-|A^1\Delta_2, v_A\rangle \\
&= \langle v_B| - B(R)|v_A\rangle\langle J\Omega = 1M|J^+|J\Omega = 2M\rangle \\
&\quad \times \sum_i \langle {}^1\Pi_1|l_i^-|{}^1\Delta_2\rangle \\
&= -[J(J+1)-2]^{1/2}\langle v_B|B(R)|v_A\rangle \\
&\quad \times \sum_i \frac{1}{2}\{\langle\sigma\alpha\delta^+\beta|l_i^-|\sigma\alpha\pi^+\beta\rangle + \langle\sigma\beta\delta^+\alpha|l_i^-|\sigma\beta\pi^+\alpha\rangle\} \\
&= -[J(J+1)-2]^{1/2}\langle v_B|B(R)|v_A\rangle \times b \\
&= \eta[J(J+1)-2]^{1/2}
\end{aligned}$$

where $b = \langle\pi^+\alpha|l^-|\delta^+\alpha\rangle = \langle\pi^+\beta|l^-|\delta^+\beta\rangle$, $\eta = -\langle v_B|B(R)|v_A\rangle \times b$.

The PGOPHER program was used to accomplish the perturbation analysis using the above matrix element. Firstly, line positions of the 0-0 band of the $A^1\Delta$-$X^1\Sigma^+$ and $B^1\Pi$-$X^1\Sigma^+$ transitions of YH and YD, together with their J assignments were inserted into the PGOPHER program. Since the lower state combination differences from the two transitions agree well with the corresponding values for the ground state from our previous studies,[15,16] the lower state spectroscopic constants were held fixed to our published values for YH (Ref. 15) and YD (Ref. 16) in the final fit. One perturbation matrix element, $\langle B^1\Pi_1, v_B|J^+L^-|A^1\Delta_2, v_A\rangle$, was included in the fit. A least-squares fit was obtained by varying spectroscopic constants for the $A^1\Delta$ and $B^1\Pi$ states and the perturbation matrix element. However, the average unweighted fitting error was around 0.05 cm^{-1}, which is about an order of magnitude larger than the experimental line position accuracy, 0.005 cm^{-1}. Trying to add more diagonal terms did not improve the fit. In order to improve the fit, the centrifugal distortion of the perturbation matrix element was introduced in the fit:

$$\begin{aligned}
&\langle B^1\Pi_1, v_B|H'_{CD}|A^1\Delta_2, v_A\rangle \\
&= \langle B^1\Pi_1, v_B|D(R)\, N^2 J^+L^-|A^1\Delta_2, v_A\rangle \\
&= \langle B^1\Pi_1, v_B|D(R)\,(J-S)^2 J^+L^-|A^1\Delta_2, v_A\rangle \\
&= J(J+1)\langle B^1\Pi_1, v_B|D(R)\, J^+L^-|A^1\Delta_2, v_A\rangle \\
&= J(J+1)[J(J+1)-2]^{1/2}\langle v_B|D(R)|v_A\rangle \\
&\quad \times \sum_i \frac{1}{2}\{\langle\sigma\alpha\delta^+\beta|l_i^-|\sigma\alpha\pi^+\beta\rangle + \langle\sigma\beta\delta^+\alpha|l_i^-|\sigma\beta\pi^+\alpha\rangle\} \\
&= J(J+1)[J(J+1)-2]^{1/2}\langle v_B|D(R)|v_A\rangle \times b \\
&= \eta_D J(J+1)[J(J+1)-2]^{1/2}
\end{aligned}$$

where $b = \langle\pi^+\alpha|l^-|\delta^+\alpha\rangle = \langle\pi^+\beta|l^-|\delta^+\beta\rangle$, $\eta_D = \langle v_B|D(R)|v_A\rangle \times b$.

After including the centrifugal distortion of the perturbation, the average unweighted fitting error was reduced to 0.006 cm^{-1}. To summarize, the following 2×2 matrix was used to model the $B^1\Pi$–$A^1\Delta$ interaction:

$$E\left(\frac{e}{f}\right) = \begin{pmatrix} E_\Delta^0 & W_{21}^{e/f} \\ W_{21}^{e/f} & E_\Pi^0 \end{pmatrix},$$

$$E_\Delta^0 = T_\Delta + B_\Delta x - D_\Delta x^2 + H_\Delta x^3 \pm \frac{1}{2}(q_{(\Delta)}x + q_{D(\Delta)}x^2),$$

$$E_\Pi^0 = T_\Pi + B_\Pi x - D_\Pi x^2 + H_\Pi x^3 + L_\Pi x^4 \pm \frac{1}{2}(q_{(\Pi)}x + q_{D(\Pi)}x^2 + q_{H(\Pi)}x^3 + q_{L(\Pi)}x^4),$$

$$W_{21}^e = (\eta + \eta_D^e x)\sqrt{x-2};\ W_{21}^f = (\eta + \eta_D^f x)\sqrt{x-2},$$

where $x = J(J+1)$; η and η_D^e/η_D^f are perturbation matrix element coefficients.

The spectroscopic constants including the interaction terms for YH and YD are provided in Tables I and II, respectively. A list of observed lines for YH and YD are deposited as

TABLE I. Spectroscopic constants (in cm^{-1}) and interaction parameters for the $A^1\Delta$ and $B^1\Pi$ states of YH.

	$A^1\Delta$		$B^1\Pi$	
Constants	v = 0	v = 1	v = 0	v = 1
T_v	9847.93880(459)	11187.1291(116)	9859.44265(452)	11201.3750(114)
B_v	4.08215(231)	4. 04880(232)	4.30866(231)	4.14664(232)
$D_v \times 10^4$	1.52721(231)	1.4596(126)	1.71023(232)	1.7175(121)
$H_v \times 10^9$	5.2826(488)	…	2.8805(666)	…
$L_v \times 10^{13}$	…	…	−4.016(162)	…
$q_v \times 10^3$	–0.0016750(936)	–0.00784(146)	1.49763(818)	1.538(47)
$q_{Dv} \times 10^5$	…	…	0.5883(112)	1.013(131)
$q_{Hv} \times 10^9$	…	…	1.6007(606)	…
$q_{Lv} \times 10^{12}$	…		1.0927(344)	…
	$A^1\Delta$ (v = 0)/$B^1\Pi$ (v = 0) Interaction		$A^1\Delta$ (v = 1)/ $B^1\Pi$ (v = 1) Interaction	
η_D^e	−0.0011921(223)		η_D^e	−0.0005341(185)
η	7.57276(178)		η	7.23057(209)
η_D^f	−0.0012374(344)		η_D^f	−0.0006181(194)

TABLE II. Spectroscopic constants (in cm^{-1}) and interaction parameters for the $A^1\Delta$ and $B^1\Pi$ states of YD.

Constants	$A^1\Delta$ v = 0	$B^1\Pi$ v = 0
T_v	9880.4094(316)	9880.9563(319)
B_v	2.0500(124)	2.2165(124)
$D_v \times 10^5$	3.584(219)	4.682(220)
$H_v \times 10^{10}$	7.566(644)	...
$q_v \times 10^4$	...	3.47(13)
$q_{Dv} \times 10^7$	...	4.49(30)
	$A^1\Delta$ (v = 0)/ $B^1\Pi$ (v = 0) Interaction	
	η_D^e	−0.000899(268)
	η	3.84480(145)
	η_D^f	−0.000904(267)

supplementary material[23] in the form of the final output of the PGOPHER program. A fit of the observed line intensities using the PGOPHER program provides a rotational temperature of 1309 ± 51 K for the YH molecule.

IV. DISCUSSION

In an extensive calculation of the spectroscopic properties of the low-lying electronic states of YH, Balasubramanian and Wang[13] have predicted the electronic states arising from the [core]$4d^15s^2$ configuration of Y and $1s^1$ configuration of H using the CASSCF with the SOCI and RCI calculations. This calculation agrees well with experimental observations.[15–19] According to this calculation the ground state of YH arises from the electron configuration, $1\sigma^2 2\sigma^2$. Some of the other very low-lying electronic states arising from the $2\sigma \rightarrow 1\delta$, $2\sigma \rightarrow 1\pi$, and $2\sigma \rightarrow 3\sigma$ electron promotions are given as follows:

$$1\sigma^2 2\sigma^1 1\delta^1 \quad A^1\Delta,\ a^3\Delta, \quad \text{(i)}$$
$$1\sigma^2 2\sigma^1 1\pi^1 \quad B^1\Pi, b^3\Pi, \quad \text{(ii)}$$
$$1\sigma^2 2\sigma^1 3\sigma^1 \quad C^1\Sigma^+, c^3\Sigma^+. \quad \text{(iii)}$$

The other higher-lying electronic states correlate with the higher energy configurations $5s^2$, $5s4d$, and $4d^2$ of the Y^+ atom.[24] Most of the higher-lying electronic states located up to 26 000 cm^{-1} have now been assigned.[15–19] Among the very low-lying electronic states, only the $X^1\Sigma^+$ and $a^3\Delta$ electronic states have been experimentally observed so far and the $b^3\Pi$, $c^3\Sigma^+$, $A^1\Delta$, and $B^1\Pi$ states remained unobserved (prior to the present work). The two new electronic transitions located near 1 μm have been assigned as $A^1\Delta$-$X^1\Sigma^+$ and $B^1\Pi$-$X^1\Sigma^+$. Although the transition from the $A^1\Delta$ state to the ground state is forbidden, this state acquires some $^1\Pi$ character because of strong interaction with the close-lying $B^1\Pi$ state and becomes allowed. The Λ-doublet splitting in v = 0 vibrational levels of the $A^1\Delta$ and $B^1\Pi$ states was calculated using their term values. The excited state term values were calculated by adding the ground state ($X^1\Sigma^+$) term values to the R or P branch lines [for the $F_e'(J)$ levels] and Q branch lines [for the $F_f'(J)$ levels] in the two 0-0 bands. In general, Λ-doublet splitting in a $^1\Delta$ state is much smaller than that in a $^1\Pi$ state and varies as $[J(J+1)]^2$, while that in a $^1\Pi$ state varies as $[J(J+1)]$. The observed splitting in the $A^1\Delta$ state is in the range of 0.0–0.15 cm^{-1} (up to J = 30) and that in the $B^1\Pi$ state lies in the range of 0.0–14.17 cm^{-1} (up to J = 36), but has an unusual J-dependence because of the perturbations. The Λ-doublet splitting in the two states is plotted with respect to J in Figure 2. In this figure the Λ-doublet splitting in the $A^1\Delta$ state is marked on the left y axis, while that in the $B^1\Pi$ state is marked on the right y axis. The electronic assignment of the $A^1\Delta$ and $B^1\Pi$ states is supported by the observed Λ-doublet splitting in the two states as shown in Figure 2.

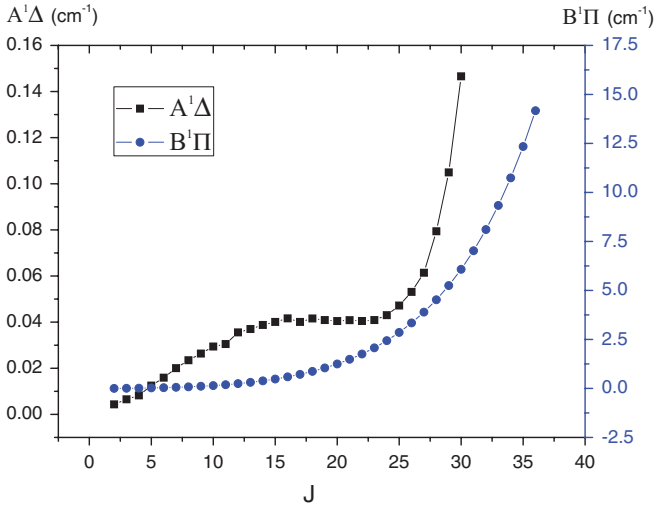

FIG. 2. A plot of Λ-doublet splitting for the $A^1\Delta$ and $B^1\Pi$ states with respect to J. The Λ-doublet splitting for the $A^1\Delta$ state is marked on the left side and that for the $B^1\Pi$ state is marked on the right side of the y axis.

As can be noticed in Tables I and II, the spectroscopic constants of the two excited state are not as well determined as expected based on the quality of the present measurements. The most probable reason for this is the use of interaction parameters to account for perturbations between the two states. These extra constants are correlated with the other parameters. The constants of Table I have been used to determine the equilibrium constants for the $A^1\Delta$ and $B^1\Pi$ states which are provided in Table III. The spectrum of YH consists of the 0-0 and 1-1 bands of the $A^1\Delta$-$X^1\Sigma^+$ and $B^1\Pi$-$X^1\Sigma^+$ transitions and no bands belonging to the $\Delta v \neq 0$ sequences were observed. Therefore, the equilibrium vibrational constants for the two excited states could not be determined. The present analysis provides $\Delta G_{1/2}$ intervals of 1339.1903(125) and 1341.9324(123) cm^{-1} for the $A^1\Delta$ and $B^1\Pi$ states, respectively. These values compare reasonably well with the

TABLE III. Equilibrium constants (in cm^{-1}) for the $A^1\Delta$ and $B^1\Pi$ states of YH.

Constants	$A^1\Delta$	$B^1\Pi$
$\Delta G(1/2)$	1339.1903(125)	1341.9324(123)
B_e	4.09883(283)	4.38967(283)
α_e	0.03335(327)	0.16201(327)
r_e(Å)	2.03153(70)	1.96308(63)

respective theoretical vibrational frequencies (ω_e) of 1366 cm^{-1} and 1380 cm^{-1}. The rotational constants for the v = 0 and 1 vibrational levels of the two states provide the equilibrium rotational constants (B_e) of 4.09883(283) cm^{-1} and 4.38967(283) cm^{-1} for the $A^1\Delta$ and $B^1\Pi$ states, respectively. These values result in the equilibrium bond lengths of 2.03153(70) Å for the $A^1\Delta$ state and 1.96308(63) Å for the $B^1\Pi$ states compared to the theoretical values of 1.95 Å and 1.944 Å, respectively. Although the observed values are somewhat larger than the theoretical values, the small difference is understandable based on the nature of calculation. For YD only the 0-0 bands were observed for the two transitions, and therefore no equilibrium parameters could be obtained for the two excited states of YD.

The rotational constants for the $A^1\Delta$ and $B^1\Pi$ states of YH and YD have been used in the traditional isotopic relation, $\rho^2 = [B/B^i]$ to check for consistency, where $\rho^2 = \mu/\mu^i$. The values of $\rho^2 = 1.9913$ and 1.9439 were derived using the rotational constants for the $A^1\Delta$ and $B^1\Pi$ states of the two isotopologues, while the calculated value is 1.9763.

We have observed small local perturbations in the v = 0 vibrational level of the $B^1\Pi$ state of YH and v = 0 vibrational level of the $A^1\Delta$ state of YD. The observed-calculated differences show that the $F_e(21)$ and $F_f(21)$ rotational levels of the $B^1\Pi$ (v = 0) state of YH and the $F_e(10)$ and F_f (13) rotational levels of the $A^1\Delta$(v = 0) state of YD are affected by interactions.

V. CONCLUSION

The emission spectra of YH and YD near 1 μm have been reinvestigated using the Fourier transform spectrometer of the National Solar Observatory at Kitt Peak. The bands observed have been assigned to two new overlapping electronic transitions, $A^1\Delta$-$X^1\Sigma^+$ and $B^1\Pi$-$X^1\Sigma^+$. The $A^1\Delta$ and $B^1\Pi$ states are about 12 cm^{-1} apart and are affected by strong interactions between the two states. A rotational analysis of the 0-0 and 1-1 bands of YH and 0-0 bands of the YD transitions has been carried out and spectroscopic constants including the interaction parameters have been determined for the two new excited states. These observations are consistent with the *ab initio* predictions of Balasubramanian and Wang.[13] A perturbation analysis has been carried out using the PGOPHER program and spectroscopic constants for the $A^1\Delta$ and $B^1\Pi$ states, including the interaction parameters, have been determined.

ACKNOWLEDGMENTS

The research described here was supported by funds from the Leverhulme Trust of UK. The spectra used in the present work were recorded by S. Johansson (deceased) at the National Solar Observatory at Kitt Peak. We would like to acknowledge Dr. Jeremy Harrison for some useful discussions on perturbations.

[1] J. N. Huiberts, R. Griessen, J. H. Rector, R. J. Wijngaarden, J. P. Dekker, D. G. de Groot, and N. J. Koeman, Nature (London) **380**, 231 (1996).
[2] W.-K. Zhang, Y.-P. Gan, X.-G. Yang, H. Huang, and L.-Y. Yu, Trans. Nonferrous Met. Soc. China **13**, 1401 (2003).
[3] T. Mongstad, C. Platzer-Björkman, S. Zh. Karazhanov, A. Holt, J. P. Maehlen, and B. C. Hauback, J. Alloys Compd. **509**, S812 (2011).
[4] A. Bernard and R. Gravina, Astrophys. J., Suppl. **52**, 443 (1983).
[5] A. Bernard and R. Gravina, Astrophys. J., Suppl. **44**, 223 (1980).
[6] A. Bernard and R. Bacis, Can. J. Phys. **55**, 1322 (1977).
[7] A. B. Kunz, M. P. Guse, and R. J. Blint, J. Phys. B **8**, L358 (1975).
[8] R. Bacis, A. Bernard, and A. Zgainsky, C. R. Hebd. Seances Acad. Sci., Ser. A, B **280**, 77 (1975).
[9] R. S. Ram and P. F. Bernath, J. Chem. Phys. **105**, 2668 (1996).
[10] R. S. Ram and P. F. Bernath, J. Mol. Spectrosc. **183**, 263 (1997).
[11] R. S. Ram and P. F. Bernath, J. Chem. Phys. **104**, 6444 (1996).
[12] S. R. Langhoff, L. G. M. Pettersson, C. W. Bauschlicher, and H. Partridge, J. Chem. Phys. **86**, 268 (1987).
[13] K. Balasubramanian and J. Z. Wang, J. Mol. Spectrosc. **133**, 82 (1989).
[14] B. Simard, W. J. Balfour, H. Niki, and P. A. Hackett, in *45th Ohio State University International Symposium on Molecular Spectroscopy, Columbus, June 11–15, Ohio, 1990*, Abstracts RC11 and RC12.
[15] R. S. Ram and P. F. Bernath, J. Chem. Phys. **101**, 9283 (1994).
[16] R. S. Ram and P. F. Bernath, J. Mol. Spectrosc. **171**, 169 (1995).
[17] X. Wang, G. V. Chertihin, and L. Andrews, J. Chem. Phys. A **106**, 9213 (2002).
[18] Z. J. Jakubek, S. Nakhate, B. Simard, and W. J. Balfour, J. Mol. Spectrosc. **211**, 135 (2002).
[19] Z. J. Jakubek, B. Simard, and W. J. Balfour, Chem. Phys. Lett. **351**, 365 (2002).
[20] B. A. Palmer and R. Engleman, *Atlas of the Thorium Spectrum* (Los Alamos National Laboratory, Los Alamos, 1983).
[21] P. F. Bernath, *Spectra of Atoms and Molecules* (Oxford University Press, New York, 2005).
[22] H. Lefebvre-Brion and R. W. Field, *The Spectra and Dynamics of Diatomic Molecules* (Elsevier/Academic Press, Amsterdam, 2004).
[23] See supplementary material at http://dx.doi.org/10.1063/1.3659295 for two tables of observed and calculated transition wavenumbers for YH and YD.
[24] A. E. Nilsson, S. Johansson, and R. L. Kurucz, Phys. Scr. **44**, 226 (1991).